Holocene slip rate of the Wasatch fault zone, Utah, from geodetic data: Earthquake cycle effects

Rocco Malservisi, Timothy H. Dixon, and Peter C. La Femina
Rosenstiel School of Marine and Atmospheric Sciences, University of Miami, USA

Kevin P. Furlong
Geodynamics Research Group, Dept. of Geosciences, The Pennsylvania State University, USA

Received 26 March 2003; revised 9 May 2003; accepted 15 May 2003; published 2 July 2003.

[1] GPS data define a broad zone of present day deformation in the eastern Basin and Range province, western US. Using finite element models with elastic upper crust over viscoelastic lower crust/upper mantle and incorporating earthquake cycle effects, we show that these data are consistent with a model whereby most contemporary fault slip is focused on the Wasatch fault zone. Modeled rates of horizontal extension are 3.0–4.5 mm/yr, in agreement with Holocene geologic data. The models are non-unique, in part because much of the Wasatch fault is in the late stages of the earthquake cycle, when surface velocity gradients across the fault are low. *INDEX TERMS:* 8123 Tectonophysics: Dynamics, seismotectonics; 8109 Tectonophysics: Continental tectonics—extensional (0905); 7223 Seismology: Seismic hazard assessment and prediction; 1206 Geodesy and Gravity: Crustal movements—interplate (8155); 1236 Geodesy and Gravity: Rheology of the lithosphere and mantle (8160). **Citation:** Malservisi, R., T. H. Dixon, P. C. La Femina, and K. P. Furlong, Holocene slip rate of the Wasatch fault zone, Utah, from geodetic data: Earthquake cycle effects, *Geophys. Res. Lett.*, *30*(13), 1673, doi:10.1029/2003GL017408, 2003.

1. Introduction

[2] Estimation of slip rates and other fault parameters from geodetic data requires assumptions about the rheology of the crust and upper mantle, to account for recoverable strain accumulation during the interseismic phase of the earthquake cycle. Elastic dislocation models are often used, as they are easy to implement and fit most geodetic data quite well. However, these models do not account for earthquake cycle effects and viscoelastic behavior of the lower crust and upper mantle [e.g., *Nur and Mavko*, 1974; *Thatcher*, 1983; *Cohen*, 1984; *Pollitz and Sacks*, 1992; *Dixon et al.*, 2003]. In this paper we investigate earthquake cycle effects on the geodetically determined deformation field around the Wasatch fault, an active, west-dipping normal fault on the eastern boundary of the Basin and Range province in western North America (Figure 1). The Wasatch fault is ideal for such studies: it has been well studied with paleoseismic techniques [*McCalpin and Nishenko*, 1996] and some constraints on crustal and upper mantle rheology are available.

0094-8276/03/2003GL017408$05.00

[3] GPS data define a broad zone of deformation across the eastern Basin and Range [*Bennett et al.*, 1998, 2002]. Conventional terrestrial geodetic data near the fault [*Savage et al.*, 1992] and GPS data up to 275 km from the fault (Figure 2) are well fit with simple elastic dislocation models, each requiring several mm/yr of slip on the Wasatch fault, in reasonable agreement with Holocene geologic observations [*Friedrich et al.*, 2003]. However, such models may misfit geodetic data farther from the fault, implying additional active structures, unmodelled processes, mismodelled rheology, or some combination. Here we show that available near-and far-field GPS data can be simultaneously fit by a simple model with realistic rheology, without appealing to additional active structures or processes, accounting for earthquake cycle effects and honoring available paleoseismic data.

2. Paleoseismologic and GPS Data

[4] The last major earthquake on the Salt Lake segment of the Wasatch fault occurred at 1230 ± 62 yr BP [*McCalpin and Nishenko*, 1996]. The weighted mean of the recurrence interval for the last four events on this segment (last 5600 years) is 1340 years. While a strictly periodic recurrence model here is an oversimplification (repeat times for individual Wasatch fault segments vary by up to a factor of two, and temporal clustering may occur; *McCalpin and Nishenko* [1996]) these data suggest that the fault is in a late stage of its earthquake cycle.

[5] Space geodetic data from sites west of the Wasatch fault and east of the Central Nevada seismic belt (Figure 1) show mainly west-directed motion relative to stable North America [*Dixon et al.*, 1995, 2000; *Bennett et al.*, 1998, 2002; *Thatcher et al.*, 1999]. We used the west velocity components of continuously operating GPS sites that span the Wasatch fault at a latitude of about 39°N [*Bennett et al.*, 2002] as far west as 115°W. Sites west of this may be affected by recent activity on other faults in the Central Nevada Seismic Belt (Figure 1). The resulting transect spans approximately 300 km, normal to the strike of the Wasatch fault. Although individual Wasatch fault segments are shorter than this (e.g., the Salt Lake segment is ~50 km long) all segments have similar strikes, and segments adjacent to the Salt Lake segment (Brigham City and Weber segments to the north, Provo and Nephi segments to the south, spanning a total of ~300 km strike length) all ruptured more than 600 years ago (i.e., all are in relatively late stages of their earthquake cycle) suggesting that simple

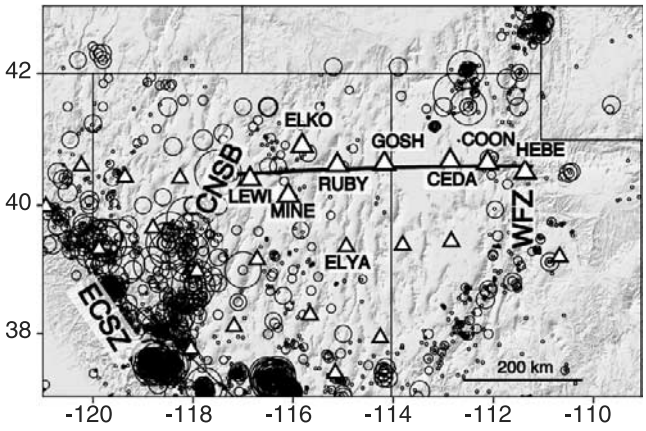

Figure 1. Regional seismicity scaled by magnitude and continuous GPS sites (triangles; [*Bennett et al.*, 2002]) in the Basin and Range province. Thick line represents transect analyzed in the paper. Sites used in this paper are marked with larger triangles and name. LEWI may be influenced by the Central Nevada Seismic Belt and it is not used in the model. ECSZ = Eastern California Shear Zone; WFZ = Wasatch Fault Zone; CNSB = Central Nevada Seismic Belt.

2-D models can provide useful approximations to the full 3-D problem.

3. Finite Element Models

[6] We model the surface velocity field associated with a normal fault locked during the interseismic period, using the finite element code TECTON [*Melosh and Raefsky*, 1980; *Govers*, 1993]. We use a two-dimensional implementation [*Govers and Meijer*, 2001] (Figure 2), incorporating rheological layering and earthquake cycle effects. The rectangular model domain is parallel to the extension direction, extending 400 km east of the fault, and 250 km to 400 km west of the fault (boundaries closer than 250 km contribute edge effects to the solution). The model domain is 70 km thick, representing the crust and most of the lithospheric mantle. The bottom boundary is free to move, to accommodate coseismic and post-seismic effects that may propagate to that depth. An elastic upper crust overlays two Maxwell viscoelastic layers (lower crust and upper mantle). The elastic layer is 25 km thick east of the Wasatch fault (Colorado Plateau) and 10 km thick west of the fault (Basin and Range) representing flexural rigidity differences suggested by gravity and topography data [*Lowry and Smith*, 1994]. We ran two classes of models, one with laterally uniform viscosity in the lower crust and upper mantle, and the other with non-uniform viscosities on each side of the fault consistent with regional studies [*Lachenbruch and Sass*, 1978; *Arabasz et al.*, 1980; *Bodel and Chapman*, 1982; *Smith and Bruhn*, 1984; *Blackwell et al.*, 1998; *Bills et al.*, 1994]. In the uniform model, the elastic layer overlies Maxwell viscoelastic material with a viscosity of 10^{19} Pa-s to a depth of 35 km, and 10^{20} Pa-s from 35 to 70 km. In the laterally varying model, the viscosity at a given depth is one order of magnitude lower west of the fault compared to east of the fault (Figure 2).

[7] *Friedrich et al.* [2003] describe five active faults on the eastern boundary of the Basin and Range up to about 85 km west of the Wasatch fault, but the Wasatch fault accommodates the majority of displacement during Holocene time. All of these faults are represented in the elastic half space model (Figure 3). However, published continuous GPS data and our finite element models are too coarse to distinguish slip on these closely spaced faults. The finite element models represent this deformation as a single fault.

[8] Finite element faults are implemented using split nodes [*Melosh and Raefsky*, 1981]. During the interseismic period, the fault is fully locked from the surface to the base of the elastic layer (10 km). Earthquakes are simulated by unlocking the fault for one time step, and displacing the crust on either side of the fault by 4 meters, consistent with paleoseismic data [*McCalpin and Nishenko*, 1996]. The earthquake is repeated with a recurrence interval such that the amount of coseismic displacement is equal to the total far field displacement. In our analysis we evaluated surface displacement after the third earthquake in the cycle; using the fourth or fifth earthquake made a negligible difference in results. However, we cannot preclude the possibility that multiple (>10) earthquakes could change the results presented here. Fault dip was fixed at 45°. We also tested dips between 30–60°. Differences in the surface velocity field near the fault occur early in the earthquake cycle for different fault dips, but results differed insignificantly from those presented here for late stages in the earthquake cycle.

[9] Gravitational effects need to be considered since density contrasts (e.g., free surface, Moho) are displaced vertically during faulting. The resulting isostatic restoring forces are simulated using Winkler restoring pressure [*Williams and Richardson*, 1991] applied at the surface and the base of the upper viscoelastic layer. During the interseismic period the model is loaded by a velocity boundary condition on the western end while the eastern side, assumed to move with stable North America, is fixed. The velocity boundary condition (equivalent to the fault's long term slip

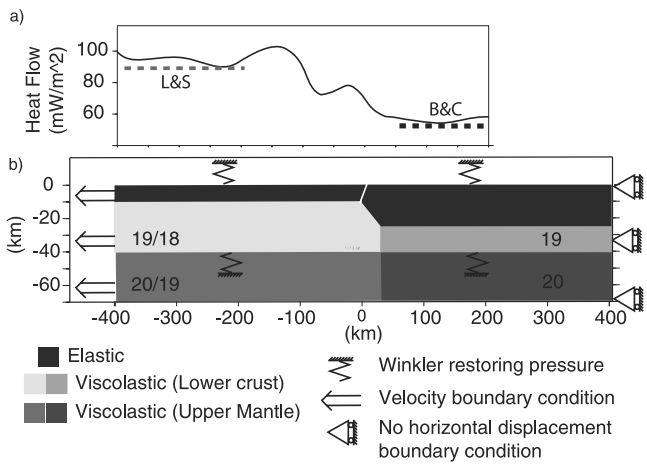

Figure 2. (a) Heat flow along modeled transect obtained by a minimum curvature interpolation of data from *Blackwell et al.* [1998]. Dashed lines are the heat flow for Colorado Plateau interior (B&C) [*Bodel and Chapman*, 1982] and the Basin and Range province (L&S) [*Lachenbruch and Sass*, 1978]. (b) Schematic representation of model, with Log (model viscosity) (Pa s) listed in each layer.

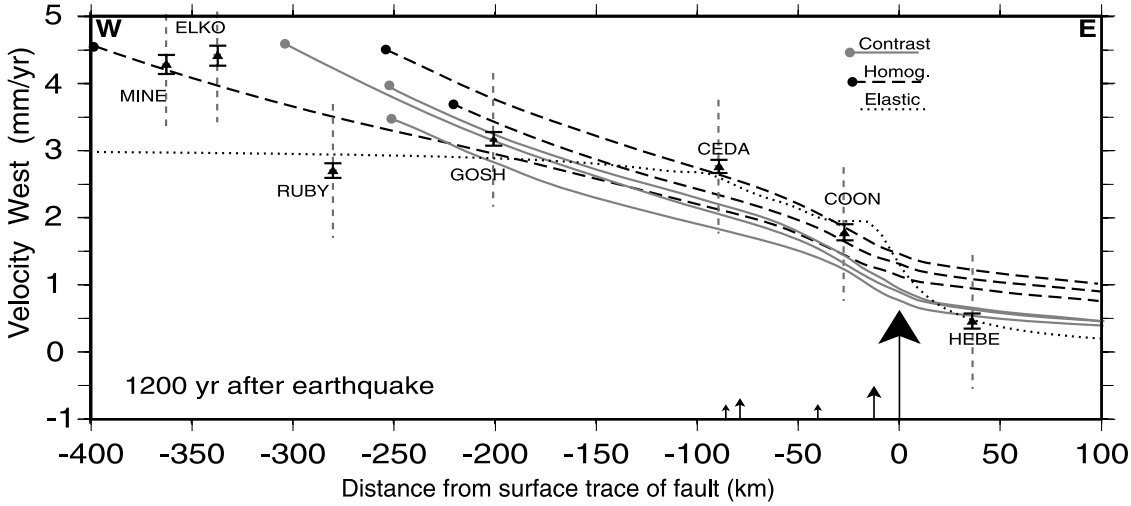

Figure 3. GPS data (triangles) with error bars assuming white noise (solid lines with crosses) and more conservative estimates incorporating reference frame and other effects (light dotted lines, *Bennett et al.* [2002]) compared to model results: 1) elastic dislocation model [e.g., *Mansinha et al.*, 1971; *Freund and Barnett*, 1976] (dotted line) assuming five faults with rates from *Friedrich et al.* [2003], all dipping 45° west, arrows at surface location, height corresponds to relative rate, locked to 10 km. Large arrow is Wasatch fault, other faults (E to W) are West Valley, Oquirrh, Stansbury, and Skull Valley; and 2) finite element models (single fault) with different velocity boundary conditions and block domains for homogeneous viscosity (dashed lines) and laterally varying viscosity (grey lines). Solid circle at end of model line indicates block size and velocity boundary condition.

rate) and block dimension are adjusted to fit the observed GPS data. Block dimension represents the region over which the strain field is dominated by the Wasatch fault; qualitatively, it can be considered to represent the distance where the fault's far field velocity is equivalent to the long-term slip rate. For the transect considered here, the velocity field starts to be influenced by the Central Nevada Seismic Belt about 400 km west of the fault (Figure 1). We considered block dimensions in the range 250–400 km west of the fault, and tested a range of slip rates equivalent to the summed Holocene rate on the Wasatch fault and nearby faults plus uncertainties. *Friedrich et al.* [2003] obtain a vertical rate for the Wasatch fault of 1.7 ± 0.5 mm/yr averaged over the last 5600 years, and a total vertical rate of 2.7 mm/yr for the five active faults in the region (Wasatch, West Valley, Oquirrh, Stansbury, and Skull Valley), with a total uncertainty of approximately 1.0 mm/yr assuming individual fault rates each have an uncertainty of 0.5 mm/yr. The corresponding horizontal rate depends on fault dip. For a typical normal fault dipping at 60°, the corresponding horizontal rate would be 1.6 mm/yr. However, there is some evidence that the Wasatch fault is a listric (low angle) fault. If all faults dipped at 30°, the summed horizontal rate would be 4.7 mm/yr. We considered rates in the range 2.0–5.0 mm/yr.

[10] A Wasatch fault earthquake was prescribed at a model time equivalent to 1200 years BP, and run to the present, consistent with paleoseismic constraints. Figure 3 shows the available GPS data and the predicted velocity fields for both uniform and laterally varying rheology models, with rates of horizontal extension between 3.0–4.5 mm/yr. Both classes of model provide acceptable fits to the data. We tested other combinations of elastic layer thicknesses (10–25 km) including a uniform thickness on each side of the fault, and different viscosities. Although details of the resulting surface velocity field differed, a common feature in all models is that high surface velocity gradients are observed near the fault in the early part of the earthquake cycle (first ~100 yrs), and then decrease as the stress relaxes, yielding an essentially linear (low gradient) velocity field in the last ~75%–85% of the earthquake cycle (Figure 4). While the Maxwell relaxation time depends on rigidity and viscosity, both assigned values in our model, the earthquake recurrence time for the Wasatch fault is sufficiently long, and the last earthquake so long ago, that for all reasonable values of rigidity and viscosity, near-field earthquake effects are completely relaxed at present, leading to low strain rates and essentially linear velocity gradients over a broad region.

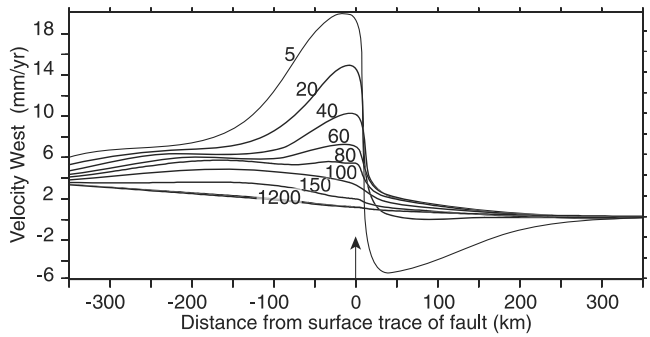

Figure 4. Velocity field along the profile at different times during the earthquake cycle for lateral contrast model; the pattern is similar for uniform rheology model. Arrow indicates surface expression of modeled fault. Note similarity of curves after about 150 years.

4. Discussion

[11] Our results are consistent with paleoseismic rate estimates for the Wasatch fault and nearby faults spanning the last 5600 years [*Freidrich et al.*, 2003]. Models with a range of slip rates (3.0–4.5 mm/yr), dips (30°–60°) and block dimensions fit the geodetic data about as well. This emphasizes the non-uniqueness of geodetic data for studies of faults late in the earthquake cycle, when velocity gradients may be low (in fact a straight line fits the data about as well as any of our models). It also suggests the importance of considering earthquake cycle effects and incorporating geologic and paleoseismic constraints when interpreting GPS or other geodetic data.

[12] *Dixon et al.* [2000] reported that a site in the central Basin and Range, ELYA, moves west relative to stable North America at 3.2 ± 1.2 mm/yr, and suggested that this represents an upper limit to the current rate of horizontal extension across the Wasatch fault. In the absence of additional active faults in the eastern Basin and Range, ELYA's velocity should approximate the longer term (e.g., Holocene) slip rate on the Wasatch fault, as it is far enough away from the fault to be essentially unaffected by elastic strain accumulation and seismic cycle effects. This ''boundary zone deformation'' model is consistent with observed patterns of seismicity, indicating significant activity around the Wasatch fault and relative quiescence in the Basin and Range interior (Figure 1). Alternately, if numerous additional active faults are present throughout the eastern Basin and Range (diffuse deformation model), ELYA's velocity represents the summed velocity contribution of all of these faults. The approximately linear, low velocity gradient observed in eastern Basin and Range GPS data might be interpreted as consistent with the latter (diffuse deformation) model. However, both the elastic dislocation model and viscoelastic finite element models (Figure 3) support a boundary zone deformation model, in agreement with Holocene paleoseismic data and previous models incorporating terrestrial geodetic data [*Savage et al.*, 1992]. Thus a broad zone of deformation may be consistent with a narrow zone of active faulting, depending on earthquake cycle stage.

[13] **Acknowledgments.** We thank Anke Friedrich for sharing results in advance of publication, Rick Bennett and two anonymous reviewers for comments on the first version of this paper, Shimon Wdowinski and Wayne Thatcher for discussions, and Shawn Larsen elastic dislocation modeling code. This work was supported by grants from NASA and NSF, including EAR 0003741 and EAR 0003396.

References

Arabasz, W., R. Smith, and W. Richins, Earthquake studies along the Wasatch front, Utah, *Bull. Seismol. Soc. Am.*, *70*, 1479–1500, 1980.

Bennett, R., B. Wernicke, and J. Davis, Continuous GPS measurements of contemporary deformation across the northern Basin and Range province, *Geophys. Res. Lett.*, *25*, 563–566, 1998.

Bennett, R., J. Davis, J. E. Normandeau, and B. P. Wernicke, Space geodetic measurements of plate boundary deformation in the western US Cordillera, in *Plate Boundary Zones*, edited by S. Stein and J. Freymueller, *AGU Geodynamics Series*, *30*, 27–55, 2002.

Bills, B., D. Curray, and G. A. Marshall, Viscosity estimates for the crust and upper mantle from lacustrine shoreline deformation, Eastern Great Basin, *J. Geophys. Res.*, *99*, 22,059–22,086, 1994.

Blackwell, D., K. Wisian, and J. Steel, Geothermal resources/reservoir investigations based on heat flow and thermal gradient data from the United States, http://www.smu.edu/~geothermal, 1998.

Bodel, J., and D. Chapman, Heat flow in north-central Colorado Plateau, *J. Geophys. Res.*, *87*, 2869–2884, 1982.

Cohen, S., Postseismic deformation due to subcrustal viscoelastic relaxation following dip-slip earthquakes, *J. Geophys. Res.*, *89*, 4538–4544, 1984.

Dixon, T., S. Robaudo, J. Lee, and M. Reheis, Constraints on present-day Basin and Range deformation from space geodesy, *Tectonics*, *14*, 755–772, 1995.

Dixon, T., M. Miller, F. Farina, H. Wang, and D. Johnson, Present-day motion of the Sierra Nevada block and some tectonic implications for the Basin and Range province, *Tectonics*, *19*, 1–24, 2000.

Dixon, T., E. Norabuena, and L. Hotaling, Paleoseismology and GPS: Earthquake-cycle effects and geodetic versus geologic fault slip rates in the Eastern California shear zone, *Geology*, *31*, 55–58, 2003.

Freund, L., and D. Barnett, A 2-D analysis of surface deformation due to dip-slip faulting, *Bull. Seismol. Soc. Am.*, *66*, 667–675, 1976.

Friedrich, A., B. Wernicke, N. Niemi, R. Bennett, and J. Davis, Comparison of geodetic and geologic data from the Wasatch region, Utah, *J. Geophys. Res.*, in press, 2003.

Govers, R., Dynamics of lithospheric extension: A modeling study, *Ph. D. thesis*, *Utrecht Univ.*, Utrecht, 240 pp., 1993.

Govers, R., and P. Meijer, On the dynamics of the Juan de Fuca plate, *Earth Planet. Sci. Lett.*, *189*, 115–131, 2001.

Lowry, A., and R. Smith, Flexural rigidity of the Basin and Range-Colorado Pleateau-Rocky Mountain transition from coherence analysis of gravity and topography, *J. Geophys. Res.*, *99*, 20,123–20,140, 1994.

Lachenbruch, A., and J. Sass, Models of an extending lithosphere and heat flow in the Basin and Range Province, *Geol. Soc. Am. Mem*, *152*, 209–250, 1978.

Mansinha, L., D. Smylie, and D. Orphal, The displacement fields of inclined faults, *Bull. Seism. Soc. Am.*, *61*, 1433–1440, 1971.

McCalpin, J., and S. Nishenko, Holocene paleoseismicity, clustering and probabilities of future large earthquakes on the Wasatch fault zone, Utah, *J. Geophys. Res.*, *101*, 6233–6253, 1996.

Melosh, H., and A. Raefsky, The dynamical origin of subduction zone topography, *Geophys. J. R. Astr. Soc.*, *60*, 333–354, 1980.

Melosh, H., and A. Raefsky, A simple and efficient method for introducing faults into finite element computations, *Bull. Seismol. Soc. Am.*, *71*, 1391–1400, 1981.

Nur, A., and G. Mavko, Postseismic viscoelastic rebound, *Science*, *183*, 204–206, 1974.

Pollitz, F., and I. Sacks, Modeling of postseismic relaxation following the great 1857 earthquake, southern California, *Bull. Seismol. Soc. Am.*, *82*, 454–480, 1992.

Savage, J., M. Lisowski, and W. Prescott, Strain accumulation across the Wasatch fault near Ogden Utah, *J. Geophys. Res.*, *97*, 2071–2083, 1992.

Smith, R., and R. Bruhn, Intraplate extensional tectonics of the eastern Basin and Range: Inferences on structural style from seismic reflection, regional tectonics, and thermal-mechanical models, *J. Geophys. Res.*, *89*, 5733–5762, 1984.

Thatcher, W., Nonlinear strain buildup and the earthquake cycle on the San Andreas fault, *J. Geophys. Res.*, *88*, 5893–5902, 1983.

Thatcher, W., G. Foulger, B. Julian, J. Svarc, E. Quilty, and G. Bawden, Present-day deformation across the Basin and Range province, Western US, *Science*, *283*, 1714–1718, 1999.

Williams, C., and R. Richardson, A rheological layered three-dimensional model of the San Andreas Fault in Central and Southern California, *J. Geophys. Res.*, *96*, 16,597–16,623, 1991.

R. Malservisi, T. H. Dixon, and P. C. La Femina, Rosenstiel School of Marine and Atmospheric Sciences, University of Miami, USA.

K. P. Furlong, Geodynamics Research Group, Dept. of Geosciences, The Pennsylvania State University, USA.